1 Report

by Gullik Vetvik Killie, Steffen Brask Add yourself

Abstract

Lorem ipsum dolor sit amet, consectetur adipisicing elit, sed do eiusmod tempor incididunt ut labore et dolore magna aliqua. Ut enim ad minim veniam, quis nostrud exercitation ullamco laboris nisi ut aliquip ex ea commodo consequat. Duis aute irure dolor in reprehenderit in voluptate velit esse cillum dolore eu fugiat nulla pariatur. Excepteur sint occaecat cupidatat non proident, sunt in culpa qui officia deserunt mollit anim id est laborum.

1.1 Introduction

Langmuir probes, as well as other instruments, are often situated outside of space crafts. The precence of the spacecraft causes disturbances to the local conditions we want to measure, these disturbances need to be corrected for. Many studies has been done on the flow of plasma around spacecraft and of the wake the spacecraft creates (Miloch, 2010; Engwall et al., 2006).

1.2 Theory

1.3 Numerical Methods

- Short PiC (EMSES) explanation
- Experimental set up
-

1.3.1 Numerical methods

To solve the problem numerically we use the EMSES code. EMSES uses the standard PIC method for plasma simulations. In the code we are able to define a spacecraft body, and the code then calculates the potential on that body using the capacitance matrix method. Although EMSES has the capability to do a full electromagnetic calculation, we have opted to use the poisson's equation solver for electrostatic problems. In the EMSES system we can define sunlit surfaces based upon an angle, and a current desity. Sunlit

surfaces will then emmit electrons based upon a energy distribution. For a complete description of EMSES' capabilities see (Nakashima et al., 2009) Parameters are choosen to simulate the sun at the earth, but with an enhanced flux to emphasize the effect in question.

1.3.2 Theoretical calculations

$$\begin{aligned} I_i =& \begin{cases} A|q|n_\infty\sqrt{\frac{8kT_i}{\pi m_i}}(without flow) \\ \frac{1}{6}A|q|n_\infty V + \frac{5}{6}A|q|n_\infty\sqrt{\frac{8kT_i}{\pi M_i}}(with flow) \end{cases} \\ I_e =& -A|q|n_\infty\sqrt{\frac{8kT_e}{\pi m_e}}exp\Big(\frac{|q|\Phi_d}{kT_e}\Big) \\ I_{ph} =& \frac{1}{6}AJ_s \end{aligned} \tag{1.1}$$

$$\begin{aligned} \Phi_d =& \frac{kT_e}{|q|}ln\Big(\sqrt{\frac{T_i}{T_e}}\sqrt{\frac{m_e}{m_i}} + \frac{J_s}{6n_\infty|q|}\sqrt{\frac{\pi m_e}{8kT_e}}\Big) + \Phi_0 \\ \Phi_d =& \frac{kT_e}{|q|}ln\Big(\frac{5}{6}\sqrt{\frac{T_i}{T_e}}\sqrt{\frac{m_e}{m_i}} + \frac{V}{6}\sqrt{\frac{\pi m_e}{8kT_e}} + \frac{J_s}{6n_\infty|q|}\sqrt{\frac{\pi m_e}{8kT_e}}\Big) \\ \Phi_0 =& kT_{ph},\ V = speed\ of\ flow \end{aligned} \tag{1.2}$$

The theory is based on thin-sheath approximation, so if SC size is much larger than Debye length of the photoelectron, we can use it.

1.3.3 Test case setup

We wish to simulate the effects of Photon emmited electrons in different test cases, and have thus set up the following 6 cases:

Case	Plasme flow	Photon emission
1:	41600 $\vec{e_x}$ m/s	0
2:	-41600 $\vec{e_z}$ m/s	0
3:	-41600 $\vec{e_y}$ m/s	0
4:	41600 $\vec{e_x}$ m/s	$-10^{-3}A/m^3$ $\vec{e_x}$
5:	-41600 $\vec{e_z}$ m/s	$-10^{-3}A/m^3$ $\vec{e_x}$
6:	-41600 $\vec{e_y}$ m/s	$-10^{-3}A/m^3$ $\vec{e_x}$

So test case 1-4, 2-5, and 3-6 are the "same" cases exept that we run the simulation with and without photon emission to compare the cases two and two.

f

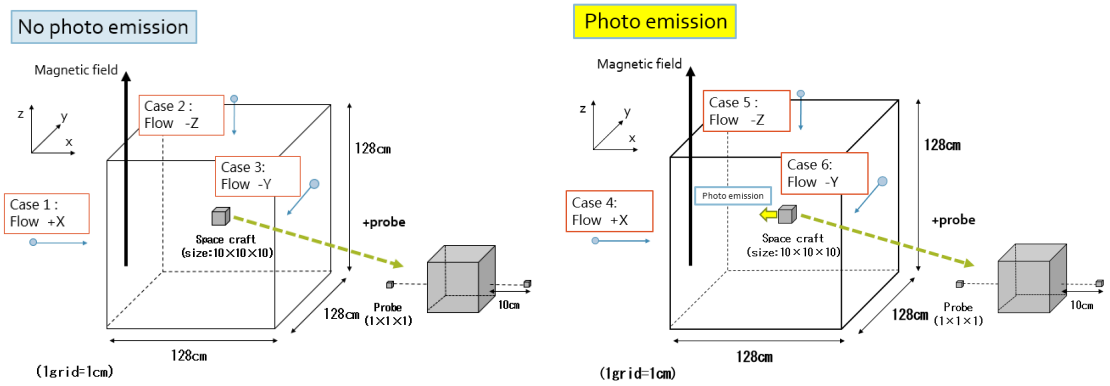

Figure 1.1: Reseach about spacecraft and surroundings without P-E and without.Left figure is no P-E simulation cases.Right figure is P-E simulation cases.

1.4 Results

1.4.1 Induced electric current

The plasma is flowing in in relation to the coordinate system in the simulations. Due to this an induced electrical field, ε, will appear. The induced electrical field will neutralize the Lorentz force. Combined with the electrostatic approximation we can obtain the ε

$$\vec{\varepsilon} = \vec{v_D} \times \vec{B} \tag{1.3}$$

This will cause a potential gradient perpendicular to the plasma flow and the magnetic field, using the electrostatic approximation we obtain the magnitude of the gradient.

$$\int E dx = -\phi \tag{1.4}$$

$$\phi = -\int \vec{v}_d \times \vec{B} \approx -\int \left(41600\text{m/s} \cdot 50E - 6\text{T}\right) dx \tag{1.5}$$

$$|\nabla\phi| = 2.08\text{m}^{-1} \tag{1.6}$$

Figure 1.2 shows the measured potential at case 6.

1.4.2 Photoemmision paths

The electrons emmited from the spacecraft due to the photoelectric effect, have a kinetic energy corresponding to a Maxwellian distribution with a temperature of $T_{ph} = 3.8481 \cdot 10^4\text{K}$. Figure 1.3 illustrates the trajectories of the emmited electrons in simulation 6. As the probes are situated 10cm to the sides of the spacecraft on the $x-$axis, the probes may be hit by the photo-emmited electrons. In the following section, **??**, we show the number of electrons hitting the probes.

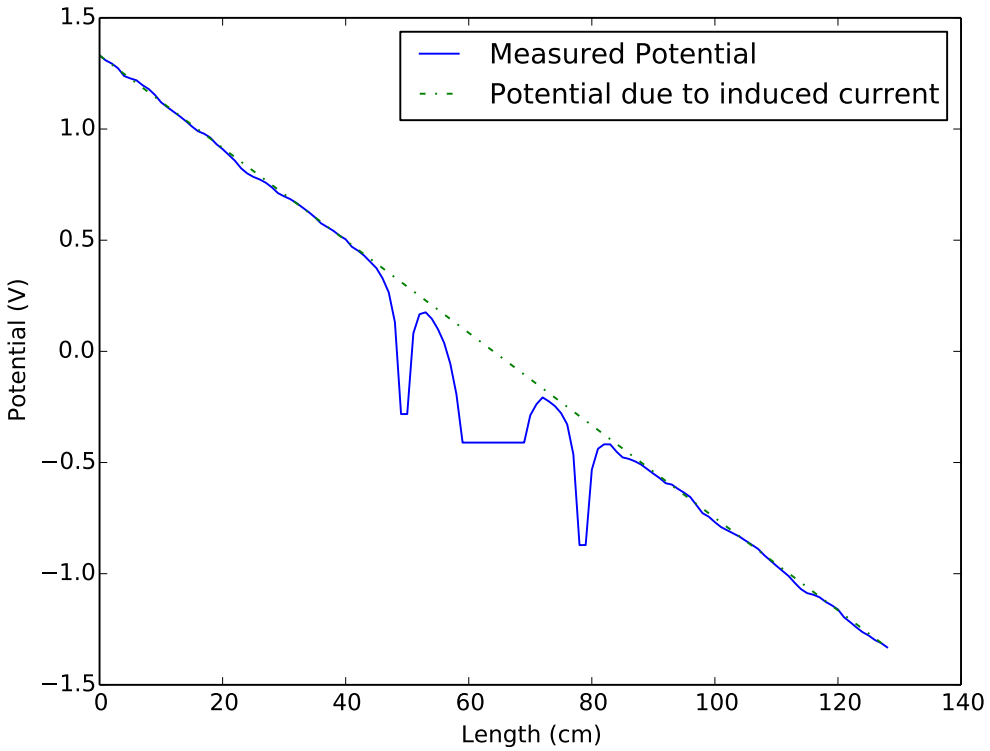

Figure 1.2: The blue line is the potential along direction x for simulation 6. In this case the potential gradient is along the $x-$axis. The dotted green line is the potential caused by the induced electrical field. This should be accounted for if we want to find the potential at the spacecraft and the probes.

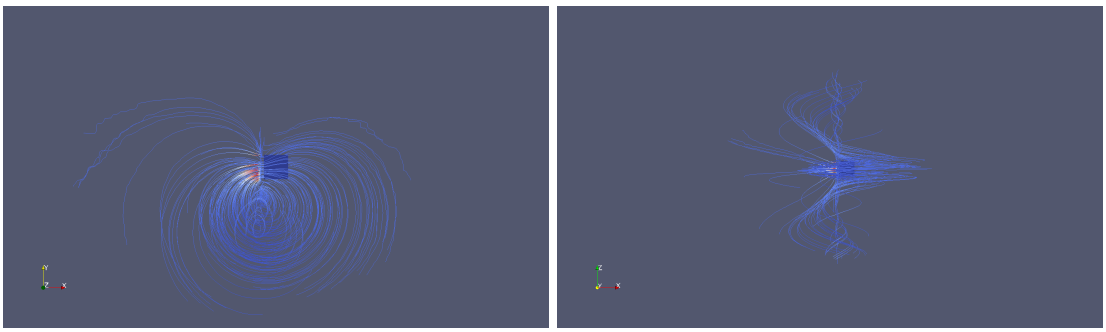

Figure 1.3: The trajectories of the electrons emmited by the photoelectric effect in simulation 6. The possible paths of the photoemmited electrons coincide with the volume occupied by the langmuir probes. The photoemmited electrons are strongly affected by the magnetic field $\vec{B}$, and follows a gyrating path guided by $\vec{B}$. The photoemmited electrons are in all the studied cases emmited from the spacecraft in $-x$ direction, and the paths are similar. The langmuir probes are situated 10cm to each side of the spacecraft along the $x-$direction. (NOTE, should have axis labels, and domain length.)

1.4.3 Accumulated Photoelectrons on Langmuir Probes

In the simulations both electrons and photoelectrons are absorbed by the probes. Table 1.4 shows the current of both regular electrons, as well as photoelectrons, interacting with the probes. The photoelectrons are emmited on the left side of the spacecraft and we see a larger current of photoelectrons here. The current caused by the photoemmision is $10 - 100$ smaller than the current from the electrons in the plasma.

	probe to +x	probe to −x
case 1	2.207E−07	2.851E−07
case 2	2.794E−07	2.807E−07
case 3	2.786E−07	2.772E−07
case 4	2.117E−07	2.609E−07
case 5	2.754E−07	2.616E−07
case 6	2.777E−07	2.512E−07

	probe to +x	probe to −x
case 4	2.3324E−09	3.49699E−08
case 5	1.9598E−09	3.51036E−08
case 6	1.3824E−09	3.66922E−08

Figure 1.4: The left table shows the electron current hitting the inserted probes at for the simulated cases $1 - 6$. On the table to the right the photoelectrons hitting the probes are shown. The photoelectron current is smaller than the electron current from the plasma, varying from $10 - 100$ times smaller.

1.4.4 Potential difference with P-E and no P-E

Case 1 vs case 4

Here we have the emitted electrons in the negative flow direction. As expected this leads to a drop in potential in the left probe which is facing the plasma flow. The potential drop over the probe is 3.8%. The right probe is now the wake where we have a drop in the ion density. This yields a large drop in potential compared to the left probe, but it also has a larger than the left probe when comparing case 1 and 4. This might be because the potential drop on the left side redirects more ions from the right side. The potential drop comparing the two cases is 10%. The potential rise over the satelite is 28%.

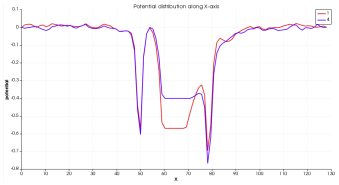

Figure 1.5: Potential of satelite and surroundings in the x-direction for case 1 and case4.

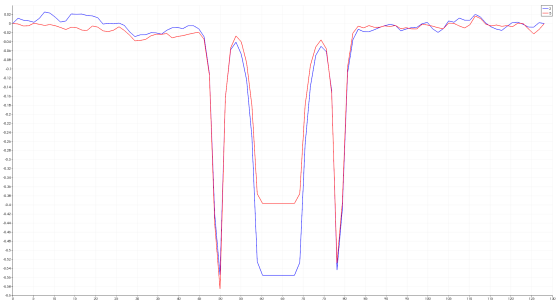

Figure 1.6: Figure show potential of satelite and surroundings in the x-direction for case 2 and 5.

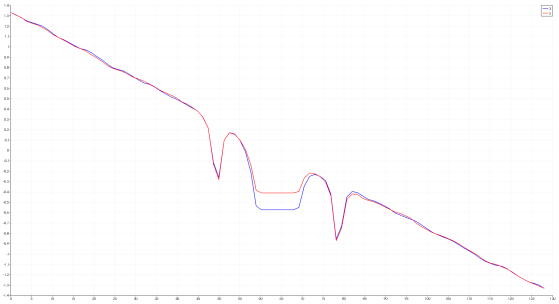

Figure 1.7: Figure show potential of satelite and surroundings in the x-direction for case 3 and 6.

Case 2 vs case 5

With the flow of emmited electrons in the negative x direction we would expect a rise in electron density around the left probe. This can be seen in figure 1.6 where we see a 5.4% drop in the potential of this probe compared to case 5 with no emitted electrons. On the right probe we have a small rise in the potential of 3.3%. With no emitted electrons on this side of the satelite the rise in potential can be explained by looking at the increase in ion density as seen in figure (need ref). In the satelite we have a potential rise of 28%. So the change in potential in the probes are small compared to the change in the satelite.

Case 3 vs case 6

A rather large drop in potential of 12% on both probes. Potential rise of 26% over the satelite.

1.4.5 Wake plots

A rather large drop in potential of 12% on both probes. Potential rise of 26% over the satelite.

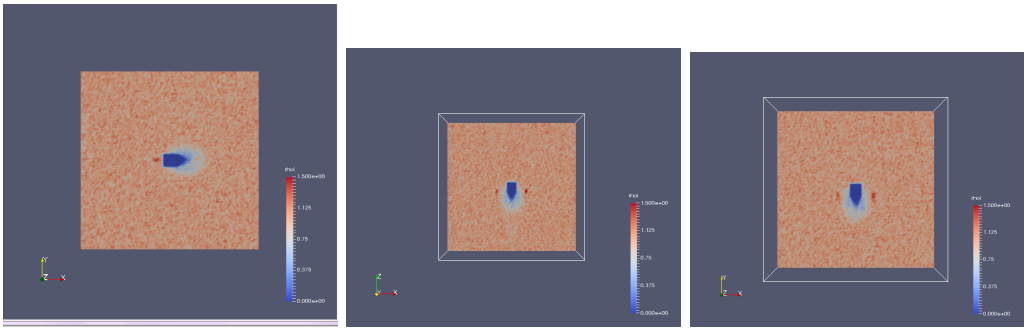

Figure 1.8: Ion density of spacecraft and surroundings without P-E Figure on the left displays case 1. Middle figure displays case 2. Rightmost figure displays case 3.

1.5 Discussion

1.6 Conclusions

- Proposal for further studies (Probably see if photoemmision is relevant in tenous plasma (MEO CASE, magnetospheric tail lobes))

Bibliography

Engwall, E. et al. (2006). "Wake formation behind positively charged spacecraft in flowing tenuous plasmas". In: *Physics of Plasmas (1994-present)* 13.6, p. 062904. ISSN: 1070-664X, 1089-7674. DOI: 10.1063/1.2199207. URL: http://scitation.aip.org/content/aip/journal/pop/13/6/10.1063/1.2199207 (visited on 27/10/2016).

Miloch, W. J. (2010). "Wake effects and Mach cones behind objects". en. In: *Plasma Physics and Controlled Fusion* 52.12, p. 124004. ISSN: 0741-3335. DOI: 10.1088/0741-3335/52/12/124004. URL: http://stacks.iop.org/0741-3335/52/i=12/a=124004 (visited on 27/10/2016).

Nakashima, H. et al. (2009). "OhHelp: a scalable domain-decomposing dynamic load balancing for particle-in-cell simulations". en. In: ACM Press, p. 90. ISBN: 978-1-60558-498-0. DOI: 10.1145/1542275.1542293. URL: http://portal.acm.org/citation.cfm?doid=1542275.1542293 (visited on 27/10/2016).